J Intell Robot Syst (2009) 54:163–181
DOI 10.1007/s10846-008-9255-0

Real-time Implementation and Validation of a New Hierarchical Path Planning Scheme of UAVs via Hardware-in-the-Loop Simulation

Dongwon Jung · Jayant Ratti · Panagiotis Tsiotras

Received: 15 March 2008 / Accepted: 30 June 2008 / Published online: 20 July 2008

Abstract We present a real-time hardware-in-the-loop simulation environment for the validation of a new hierarchical path planning and control algorithm for a small fixed-wing unmanned aerial vehicle (UAV). The complete control algorithm is validated through on-board, real-time implementation on a small autopilot having limited computational resources. We present two distinct real-time software frameworks for implementing the overall control architecture, including path planning, path smoothing, and path following. We emphasize, in particular, the use of a real-time kernel, which is shown to be an effective and robust way to accomplish real-time operation of small UAVs under non-trivial scenarios. By seamless integration of the whole control hierarchy using the real-time kernel, we demonstrate the soundness of the approach. The UAV equipped with a small autopilot, despite its limited computational resources, manages to accomplish sophisticated unsupervised navigation to the target, while autonomously avoiding obstacles.

Keywords Path planning and control · Hardware-in-the-loop simulation (HILS) · UAV

1 Introduction

Autonomous, unmanned ground, sea, and air vehicles have become indispensable both in the civilian and military sectors. Current military operations, in particular,

D. Jung (✉) · J. Ratti · P. Tsiotras
Georgia Institute of Technology, Atlanta, GA 30332-0150, USA
e-mail: dongwon.jung@gatech.edu

J. Ratti
e-mail: jayantratti@gatech.edu

P. Tsiotras
e-mail: tsiotras@gatech.edu

depend on a diverse fleet of unmanned (primarily aerial) vehicles that provide constant and persistent monitoring, surveillance, communications, and–in some cases–even weapon delivery. This trend will continue, as new paradigms for their use are being proposed by military planners. Unmanned vehicles are also used extensively in civilian applications, such as law enforcement, humanitarian missions, natural disaster relief efforts, etc.

During the past decade, in particular, there has been an explosion of research related to the control of small unmanned aerial vehicles (UAVs). The major part of this work has been conducted in academia [3–5, 10, 13–15, 23–25], since these platforms offer an excellent avenue for students to be involved in the design and testing of sophisticated navigation and guidance algorithms [17].

The operation of small-scale UAVs brings about new challenges that are absent in their large-scale counterparts. For instance, *autonomous* operation of small-scale UAVs requires both trajectory design (planning) and trajectory tracking (control) tasks to be completely automated. Given the short response time scales of these vehicles, these are challenging tasks using existing route optimizers. On-board, real-time path planning is especially challenging for small UAVs, which may not have the on-board computational capabilities (CPU and memory) to implement some of the sophisticated path planning algorithms proposed in the literature. In fact, the effect of limited computational resources on the control design of real-time, embedded systems has only recently received some attention in the literature [1, 29]. The problem is exacerbated when a low-cost micro-controller is utilized as an embedded control computer.

Autonomous path planning and control for small UAVs imposes severe restrictions on control algorithm development, stemming from the limitations imposed by the on-board hardware and the requirement for real-time implementation. In order to overcome these limitations it is imperative to develop computationally efficient algorithms that make use of the on-board computational resources wisely.

Due to the stringent operational requirements and the hardware restrictions imposed on the small UAVs, a complete solution to fully automated, unsupervised, path planning and control of UAVs remains a difficult undertaking. Hierarchical structures have been successfully applied in many cases in order to deal with the issue of complexity. In such hierarchical structures the entire control problem is subdivided into a set of smaller sub-control tasks (see Fig. 1). This allows for a more straightforward design of the control algorithms for each modular control task. It also leads to simple and effective implementation in practice [2, 27, 28].

In this paper, a complete solution to the hierarchical path planning and control algorithm, recently developed by the authors in Refs. [16, 21, 30], is experimentally validated on a small-size UAV autopilot. The control hierarchy consists of path planning, path smoothing, and path following tasks. Each stage provides the necessary commands to the next control stage in order to accomplish the goal of the mission, specified at the top level. The execution of the entire control algorithm is demonstrated through a realistic hardware-in-the-loop (HIL) simulation environment. All control algorithms are coded on a micro-controller running a real-time kernel, which schedules each task efficiently, by taking full advantage of the provided kernel services. We describe the practical issues associated with the implementation of the proposed control algorithm, while taking into consideration the actual hardware limitations.

We emphasize the use of a real-time kernel for implementing the overall control architecture. A real-time operating system provides the user with great flexibility in building complex real-time applications [11], owing to the ease in programming, error-free coding, and execution robustness. We note in passing that currently there exist many real-time kernels employed for real-time operation of UAVs. They differ in the kernel size, memory requirements, kernel services, etc. Some of these real-time kernels can be adopted for small micro-controller/processor [6, 12]. An open source real-time Linux is used for flight testing for UAVs [8]. In this work we have used the MicroC/OS-II [26], which is ideal for the small microcontroller of our autopilot.

2 Hierarchical Path Planning and Control Algorithm

In this section, we briefly describe a hierarchical path planning and control algorithm, which has been recently developed by the authors, and which takes into account the limited computational resources of the on-board autopilot.

Figure 1 shows the overall control hierarchy. It consists of path planning, path smoothing, path following, and the low level autopilot functions. At the top level of the control hierarchy, a wavelet-based, multiresolution path planning algorithm [21, 30] is employed to compute an optimal path from the current position of

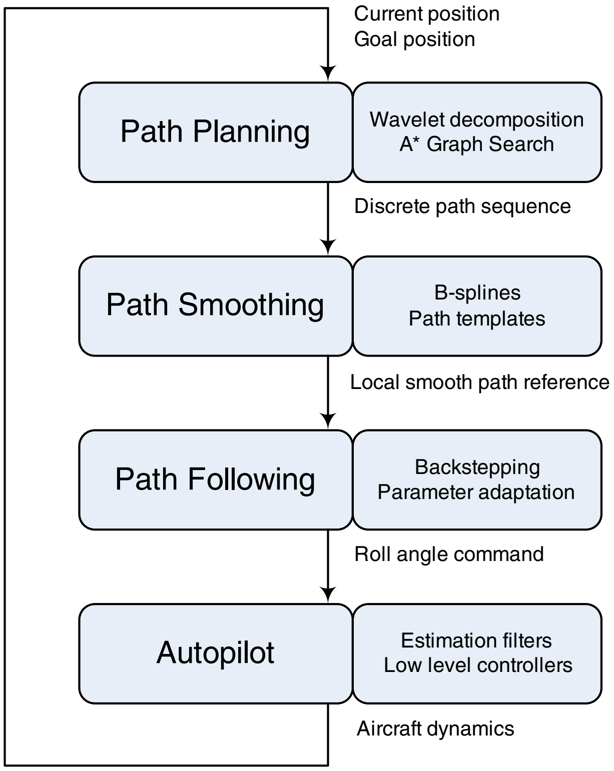

Fig. 1 Block diagram of the hierarchy of proposed control algorithm

the vehicle to the goal. The path planning algorithm utilizes a multiresolution decomposition of the environment, such that a coarser resolution is used far away from the agent, whereas fine resolution is used in the vicinity of the agent. The result is a topological graph of the environment of known a priori complexity. The algorithm then computes a path with the highest accuracy at the current location of the vehicle, where is needed most. Figure 2 illustrates this idea. In conjunction with the adjacency relationship derived directly from the wavelet coefficients [21], a discrete cell sequence (i.e., channel) to the goal destination is generated by invoking the $\mathcal{A}^*$ graph search algorithm [7, 9].

The discrete path sequence is subsequently utilized by the on-line path smoothing layer to generate a smooth reference path, which incorporates path templates comprised of a set of B-spline curves [22]. The path templates are obtained from an off-line optimization step, so that the resulting path is ensured to stay inside the prescribed cell channel. The on-line implementation of the path smoothing algorithm finds the corresponding path segments over a finite planning horizon with respect to the current position of the agent, and stitches them together, while preserving the smoothness of the composite curve.

After a local smooth reference path is obtained, a nonlinear path following control algorithm [20] is applied to asymptotically follow the reference path constructed by the path smoothing step. Assuming that the air speed and the altitude of the UAV are constant, a kinematic model is utilized to design a control law to command heading rate. Subsequently, a roll command to follow the desired heading rate is computed by taking into account the inaccurate system time constant. Finally, an autopilot with on-board sensors that provides feedback control for the attitude angles, air speed, and altitude, implements the low-level inner loops for command following to attain the required roll angle steering, while keeping the altitude and the air speed constant.

As shown in Fig. 1, at each stage of the hierarchy, the corresponding control commands are obtained from the output of the previous stage, given the initial

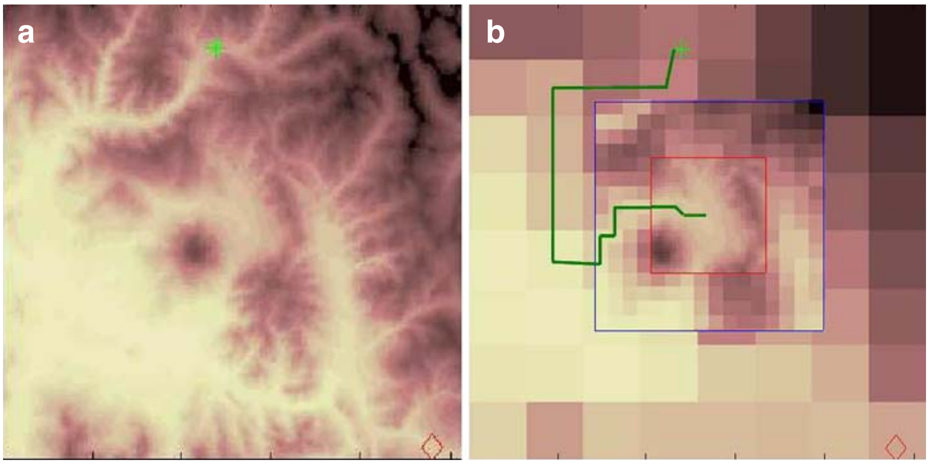

Fig. 2 Demonstration of multi-resolution decomposition of the environment (**a**) using square cells induced by the use of Haar wavelets (**b**). The current location of the agent (vehicle) is at the center of the red square (high-resolution region). The dynamics are included in the high-resolution region

environment information (e.g., a two dimensional elevation map). With the goal position specified by the user, this hierarchical control algorithm allows the vehicle to accomplish its mission of reaching the goal destination, while avoiding obstacles.

3 Experimental Test-Bed

3.1 Hardware Description

A UAV platform based on the airframe of an off-the-shelf R/C model airplane has been developed to implement the hierarchical path planning and control algorithm described above. The development of the hardware and software was done completely in-house. The on-board autopilot is equipped with a micro-controller, sensors and actuators, and communication devices that allow full functionality for autonomous control. The on-board sensors include angular rate sensors for all three axes, accelerometers along all three axes, a three-axis magnetic compass, a GPS sensor, and absolute and differential pressure sensors. An 8-bit micro-controller (Rabbit RCM-3400 running at 30 MHz with 512 KB RAM and 512 KB Flash ROM) is the core of the autopilot. The Rabbit RCM-3400 is a low-end micro-controller with limited computational throughput (as low as 7 μs for floating-point multiplication and 20 μs for computing a square root) compared to a generic high performance 32 bit micro-processor. This micro-controller provides data acquisition, data processing, and manages the communication with the ground station. It also runs the estimation algorithms for attitude and absolute position and the low-level control loops for the attitude angles, air speed, and altitude control. A detailed description of the UAV platform and the autopilot can be found in Refs. [17, 18].

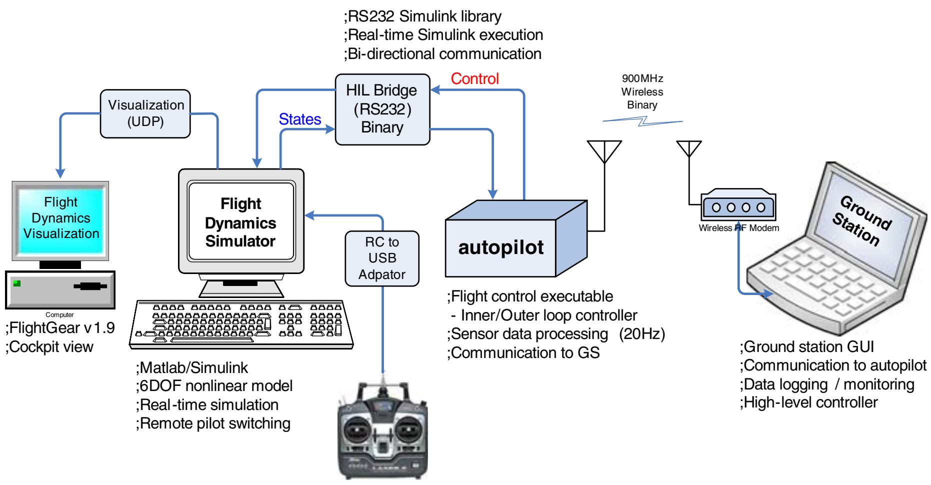

Fig. 3 High fidelity hardware-in-the-loop simulation (HILS) environment for rapid testing of the path planning and control algorithm

3.2 Hardware-in-the-Loop Simulation Environment

A realistic hardware-in-the-loop simulation (HILS) environment has been developed to validate the UAV autopilot hardware and software operations utilizing Matlab® and Simulink®. A full 6-DOF nonlinear aircraft model is used in conjunction with a linear approximation of the aerodynamic forces and moments, along with gravitational (WGS-84) and magnetic field models for the Earth. Detailed models of the sensors and actuators have also been incorporated. Four independent computers are used in the HILS, as illustrated in Fig. 3. A 6-DOF simulator, a flight visualization computer, the autopilot micro-controller, and the ground station computer console are involved in the HIL simulation. Further details about the HILS set-up can be found in Ref. [19].

4 Real-Time Software Environment

The software architecture of the on-board autopilot is shown in Fig. 4. It is comprised of several blocks, called *tasks*, which are allotted throughout different functioning layers such as the application level, the low level control, the data processing level, and the hardware level. The tasks at the hardware level, or hardware services, interact with the actual hardware devices to collect data from the sensors, communicate with the ground station, and issue commands to the DC servo motors. The

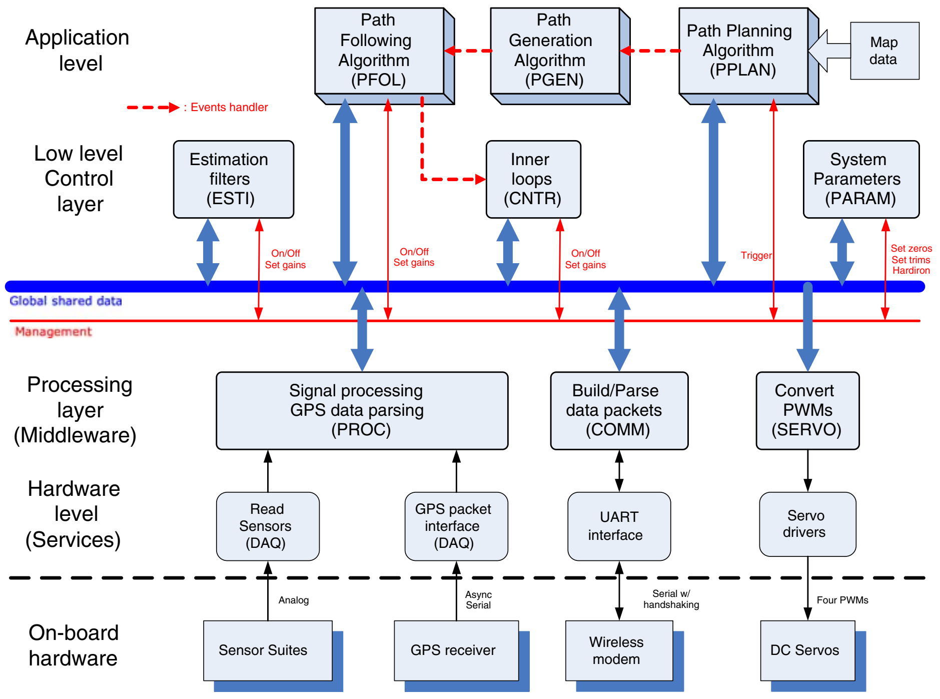

Fig. 4 Software architecture of the on-board autopilot system of the fixed-wing UAV

middleware tasks on top of the hardware services provide the abstraction of the inbound and outbound data, by supplying the processed data on a globally shared data bus or by extracting data from the global bus to the corresponding hardware services. Utilizing the processed data on the globally shared data bus, the lower level control layer achieves the basic control functions such as estimation of the attitude angles, estimation of the absolute position, and implementation of the inner loop PID controllers. Finally, three application tasks, which correspond to path planning, path generation, and path following, are incorporated to implement the hierarchical control architecture described in Section 2. The hierarchical control structure dictates all application tasks, in the sense that completion of the upper level task (event triggered) initiates the execution of a lower level task (event processed). This is shown by red dashed arrows in Fig. 4 each representing an event signal. In Fig. 4, besides exchanging the data via the global shared data bus, each task is managed by a global management bus, used for triggering execution of tasks, initializing/modifying system parameters, etc.

The task management, also called task scheduling, is the most crucial component of a real-time system. It seamlessly integrates the multiple "tasks" in this real-time software application. In practice however, a processor can only execute one instruction at a time; thus multitasking scheduling is necessitated for embedded control system implementations where several tasks need to be executed while meeting real-time constraints. Using multitasking, more than one task, such as control algorithm implementation, hardware device interfaces and so on, can appear to be executed in parallel. However, the tasks need to be prioritized based on their importance in the software flow structure so that the multitasking kernel correctly times their order of operation, while limiting any deadlocks or priority inversions.

4.1 Cooperative Scheduling Method: Initial Design

For the initial implementation, we developed a near real-time control software environment that is based predominately on the idea of cooperative scheduling. Cooperative scheduling is better explained by a large main loop containing small fragments of codes (tasks). Each task is configured to voluntarily relinquish the CPU when it is waiting, allowing other tasks to execute. This way, one big loop can execute several tasks in parallel, while no single task is busy waiting.

Like most real-time control problems, we let the main loop begin while waiting for a trigger signal from a timer, as shown by the red arrows in Fig. 5. In accordance with the software framework of Fig. 4, we classify the tasks into three groups: *routine tasks, application tasks*, and *non-periodic tasks*. The routine tasks are critical tasks required for the UAV to perform minimum automatic control. In our case these consist of the tasks of reading analog/GPS sensors (DAQ), signal processing (PROC), estimation (ESTI), inner loop control (CNTR), and servo driving (SERVO). The sampling period T_s is carefully chosen to ensure the completion of the routine tasks and allow the minimum sampling period to capture the fastest dynamics of the system. In order to attain real-time scheduling over all other tasks besides the routine tasks, a sampling period of $T_s = 50$ ms, or a sampling rate of 20 Hz, was used. On the other hand, some of the application tasks require substantial computation time and resources, as they deal with the more complicated, high level computational algorithms such as path planning (PPLAN), path generation (PGEN), and path

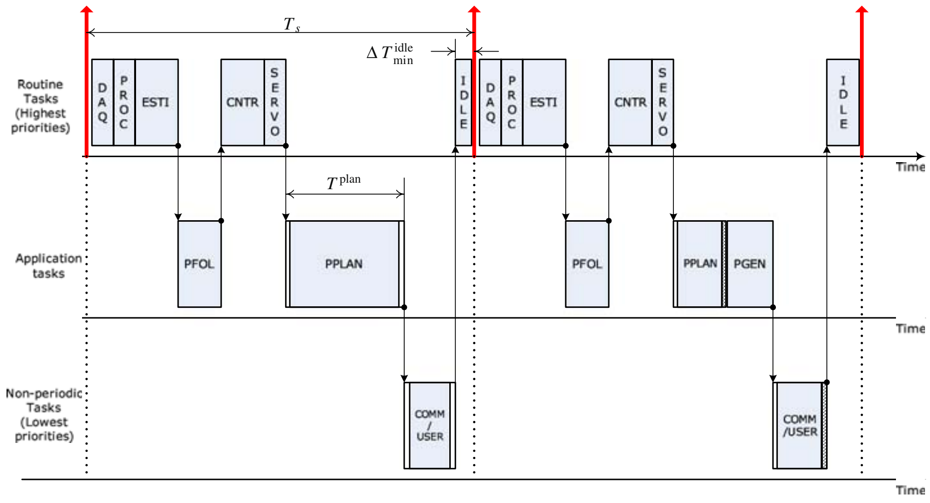
T_s
$\Delta T^{\text{idle}}_{\text{min}}$
Routine Tasks (Highest priorities)
DAQ
PROC
ESTI
CNTR
SERVO
IDLE
Time
T^{plan}
Application tasks
PFOL
PPLAN
PGEN
Non-periodic Tasks (Lowest priorities)
COMM / USER

Fig. 5 A real-time scheduling method combining cooperative and naive preemptive multitasking

following (PFOL). In particular, the path planning algorithm in Ref. [21] turns out to have a total computation time greater than the chosen sampling period. As a result, and in order to meet the real-time constraints, we fragmentized the execution of the computationally intensive task, PPLAN into several slices of code execution, each with a finite execution time T^{plan}. The finite execution time is selected a priori by taking into account both T_s and the (estimated) total execution time of the routine tasks. The objective is to maximize the CPU usage to complete the task PPLAN as soon as possible, while meeting the criterion for real-time operation. Finally, non-periodic tasks such as communication (COMM) and user application (USER) are executed whenever the CPU becomes available, ensuring a minimum idling time of duration $\Delta T^{\text{idle}}_{\text{min}}$ to allow the CPU to wait for other triggering signals.

Figure 6 shows a pseudo-code implementation of the cooperative scheduling scheme. Each `costate` implements the cooperative scheduling, while the `slice` statement implements the naive preemptive scheduling, which preempts the CPU over the finite execution window T^{plan}.

4.2 Preemptive Scheduling Method: Final Design

Given the a priori knowledge of the required tasks to be executed, in conjunction with an approximate knowledge of the total execution time, the use of *costate* blocks was shown to be an effective implementation of cooperative scheduling in the previous section. However, it is often a painstaking job for a programmer to meticulously synchronize and schedule all tasks in the application, many of which may have unpredictable execution time. Alternatively, it is possible to design a cooperative scheduler using conservative timing estimates for the corresponding tasks in a manner similar to that of Section 4.1. However, such an approach will result in poor performance in terms of the overall completion time. With a conservative estimate of execution times for the routine tasks, the portion allotted for the

Fig. 6 Pseudo-code implementation of the combined cooperative/preemptive scheduling scheme for the hierarchical path planning and control algorithm

```
main() {
    while (1) {
        costate {
            Wait_for_timer ($T_s$);
            Task DAQ;
            Task PROC;
            Task ESTI;
            if (EVENT(PFOL)) Task CNTR;
            Task SERVO;
        }
        costate {
            if (EVENT(PGEN)) Task PFOL;
        }
        costate {
            if (EVENT(PPLAN)) Task PGEN;
        }
        costate {
            Task COMM;
            Task PARAM;
            Task USER;
        }
        if ($\Delta T^{\text{idle}} > \Delta T^{\text{plan}}$) {
            slice ($\Delta T^{\text{plan}}$, Task PPLAN);
        }
    }
}
```

execution of the computationally expensive tasks remains fixed regardless whether the CPU remains idle for the rest of the sampling period. This implies that the CPU does not make full use of its capacity, thus delaying the execution of the overall tasks by a noticeable amount of time. The throughput of the computationally intensive tasks may be improved by employing a *preemptive multitasking scheduler* [26]. Since the kernel has full access to CPU timing, it can allot the CPU resources to the lower level tasks whenever the higher level tasks relinquish their control. This effectively minimizes the CPU idle time and reduces the task completion time. In the next section we present an alternative framework for implementing the hierarchical path planning and control algorithm shown in Section 2 using a preemptive real-time kernel, namely, MicroC/OS-II.

The MicroC/OS-II is known to be a highly portable, low on memory, scalable, preemptive, real-time operating system for small microcontrollers [26]. Besides being a preemptive task scheduler which can manage up to 64 tasks, the MicroC/OS-II also provides general kernel services such as semaphores, including mutual exclusion semaphores, event flags, message mailboxes, etc. These services are especially helpful for a programmer to build a complex real-time software system and integrate tasks seamlessly. Its use also simplifies the software structure by utilizing a state flow concept. The MicroC/OS-II allows small on-chip code size of the real-time kernel. The code size of the kernel is no more than approximately 5 to 10 kBytes [26], adding a relatively small overhead (around 5.26%) to the current total code size of 190 kBytes for our application.

4.2.1 Real-time software architecture

Real-time software programming begins with creating a list of tasks. In this work we emphasize the real-time implementation of the path planning and control algorithm using HILS. This requires new tasks to deal with the additional HILS communication. The simulator transmits the emulated sensor data to the micro-controller via serial communication. Hence, the sensor/GPS reading task (DAQ) is substituted with the sensor data reading task (HILS_Rx), which continuously checks a serial buffer for incoming communication packets. Similarly, the servo driving task (SERVO) is replaced by the command writing task (HILS_Tx), which sends back PWM servo commands to the simulator. On the other hand, the communication task COMM is subdivided into three different tasks according to their respective roles, such as a downlink task for data logging (COMM_Tx), an uplink task for user command (COMM_Rx), and a user command parsing task (COMM_Proc). In addition, we create a path management (PMAN) task which coordinates the execution of the path planning and control algorithm, thus directly communicating with PPLAN, PGEN, and PFOL, respectively. Finally, a run-time statistics checking task (STAT) is created in order to obtain run-time statistics of the program such as CPU usage and the execution time of each task. These can be used to benchmark the performance of the real-time kernel. Table 1 lists all tasks created in the real-time kernel.

The MicroC/OS-II manages up to 64 distinct tasks, the priorities of which must be uniquely assigned. Starting from zero, increasing numbers impose lower priorities to be assigned to corresponding tasks. In particular, because the top and bottom ends of the priority list are reserved for internal kernel use, application tasks are required to have priorities other than a priority level in this protected range. Following an empirical convention of priority assignment, we assign the critical tasks with high priorities because they usually involve direct hardware interface. In order to minimize degradation of the overall performance of the system, the hardware

Table 1 List of tasks created by the real-time kernel

ID	Alias	Description	Priority
1	HILS_Tx	Sending back servo commands to the simulator	11
2	HILS_Rx	Reading sensor/GPS packets from the simulator	12
3	COMM_Rx	Uplink for user command from the ground station	13
4	COMM_Proc	Parsing the user command	14
5	ESTI_Atti	Attitude estimation task	15
6	ESTI_Nav	Absolute position estimation task	16
7	CNTR	Inner loop control task	17
8	PFOL	Nonlinear path following control task	18
9	COMM_Tx	Downlink to the ground station	19
10	PGEN	Path generation task using B-spline templates	20
11	PMAN	Control coordination task	21
13	PPLAN	Multiresolution path planning task	23
12	STAT	Obtaining run-time statistics	22

related tasks may need proper synchronization with the hardware, hence demanding immediate attention. It follows that routine tasks that are required for the UAV to perform minimum automatic control such as ESTI_Atti, ESTI_Nav, and CNTR are given lower priorities. Finally, application-specific tasks such as PFOL, PGEN, and PPLAN are given even lower priorities. This implies that these tasks can be activated whenever the highest priority tasks relinquish the CPU. Table 1 shows the assigned priority for each task. Note that the task COMM_Tx is assigned with a lower priority because this task is less critical to the autonomous operation of the UAV.

Having the required tasks created, we proceed to design a real-time software framework by establishing the relationships between the tasks using the available kernel services: A semaphore is utilized to control access to a globally shared object in order to prevent it from being shared indiscriminately by several different tasks. Event flags are used when a task needs to be synchronized with the occurrence of multiple events or relevant tasks. For inter-task communication, a mailbox is employed to exchange a message in order to convey information between tasks.

Figure 7 illustrates the overall real-time software architecture for the autopilot. In the diagram two binary semaphores are utilized for two different objects corresponding to the wireless modem and a reference path curve, respectively. Any task that requires getting access to those objects needs to be blocked (by semaphore pending) until the corresponding semaphore is either non-zero or is released (by semaphore posting). Consequently, only one task has exclusive access to the objects at a time, which allows data compatibility among different tasks. The event flags are posted by the triggering tasks and are consumed by the pending tasks, allowing synchronization of two consecutive tasks. Note that an event from the HILS_Rx triggers a chain of routine tasks for processing raw sensor data (ESTI_Atti, ESTI_Nav) and control implementation (CNTR). A global data storage is used to hold all significant variables that can be referenced by any task, while the global flags declaration block contains a number of event flag groups used for synchronization of tasks. Each mailbox can hold a byte-length message which is posted by a sender task with information indicated next to the data flow arrow symbol. Each task receiving the message will empty the mailbox and wait for another message to be posted. These mailboxes are employed to pass the results of one task to another task. It should be noted that when the task PMAN triggers the task PPLAN, the results of subsequent tasks are transmitted via mailboxes in the following order: (PPLAN $\rightarrow$ PGEN $\rightarrow$ PMAN $\rightarrow$ PFOL).

4.2.2 Benefits of using a real-time kernel

Robustness: The real-time kernel provides many error handling capabilities during deadlock situations. We have been able to resolve all possible deadlocks using the timing features of the Semaphore-Pend or Flag-Pend operations. The kernel provides time-out signals in the semaphore and flag calls with appropriate generated errors. These are used to handle the unexpected latency or deadlock in the scheduling operation.

Flexibility and ease of maintenance: The entire architecture for the autopilot software has been designed, while keeping in mind the object-oriented requirements for an applications engineer. The real-time kernel provides an easy and natural way to achieve this goal. The architecture has been designed to keep the code flexible enough to allow adding higher level tasks, like the ones required to process

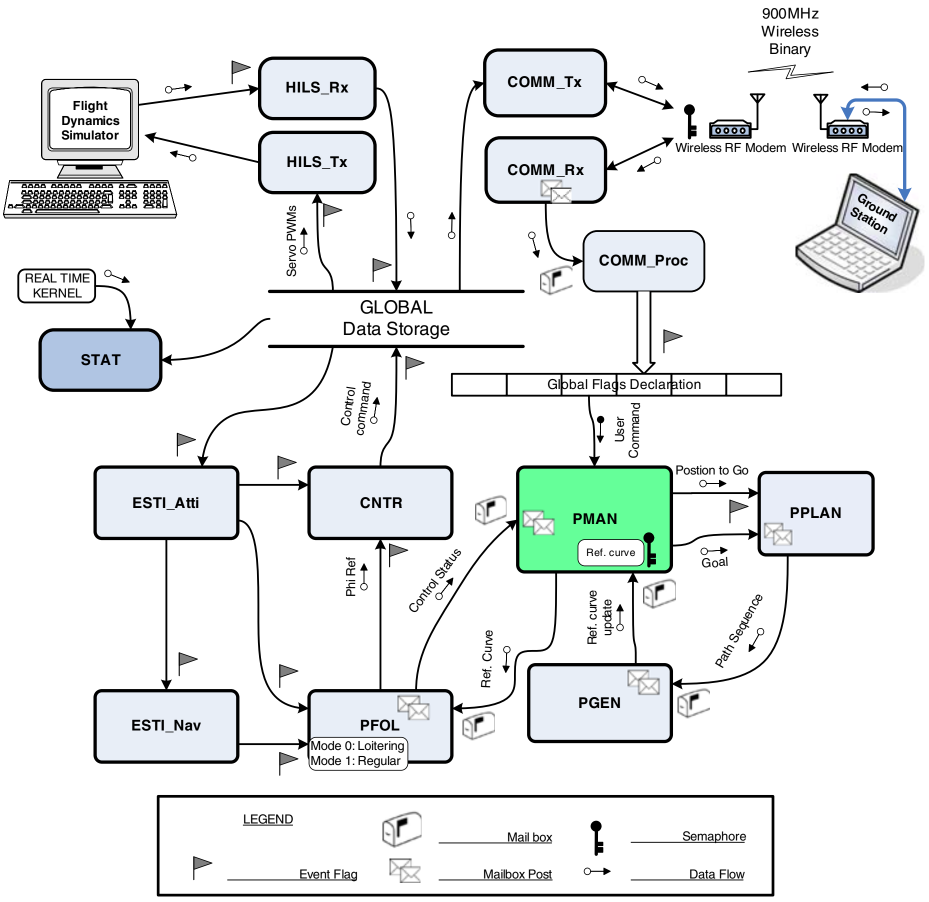

Fig. 7 The complete real-time software architecture for the path planning and control of the UAV

and execute the multi-resolution wavelet path planning algorithm. All this can be achieved without engrossing into the system level intricacies of handling and programming a microcontroller/microprocessor. The flexibility of the architecture also makes it extremely efficient to debug faults in low-level, mid-level or high-level tasks, without having to re-code/interfere with the other tasks.

5 Hardware-in-the-Loop Simulation Results

In this section we present the results of the hierarchical path control algorithm using a small micro-controller in a real-time HILS environment. The details of the implementation are discussed in the sequel.

5.1 Simulation Scenario

The environment is a square area containing actual elevation data of a US state, of dimension 128×128 units, which corresponds to 9.6×9.6 km. Taking into account the available memory of the micro-controller, we choose the range and granularity of the fine and coarse resolution levels. Cells at the fine resolution have dimensions 150×150 m, which is larger than the minimum turning radius of the UAV. The minimum turn radius is approximately calculated for the vehicle flying at a constant speed of $V_T = 20$ m/s with a bounded roll angle of $|\phi| \leq 30°$, resulting in a minimum turn radius of $R_{\min} \approx 70$ m.

The objective of the UAV is to generate and track a path from the initial position to the final position while circumventing all obstacles above a certain elevation threshold. Figure 8 illustrates the detailed implementation of the proposed path planning and control algorithm. Initially, the UAV is loitering around the initial position $\boldsymbol{p}_0$ until a local path segment from $\boldsymbol{p}_0$ to $\boldsymbol{p}_a$ is computed (Step A,B). Subsequently, the path following controller is engaged to follow the path (Step C,D). At step D, the UAV replans to compute a new path from the intermediate location

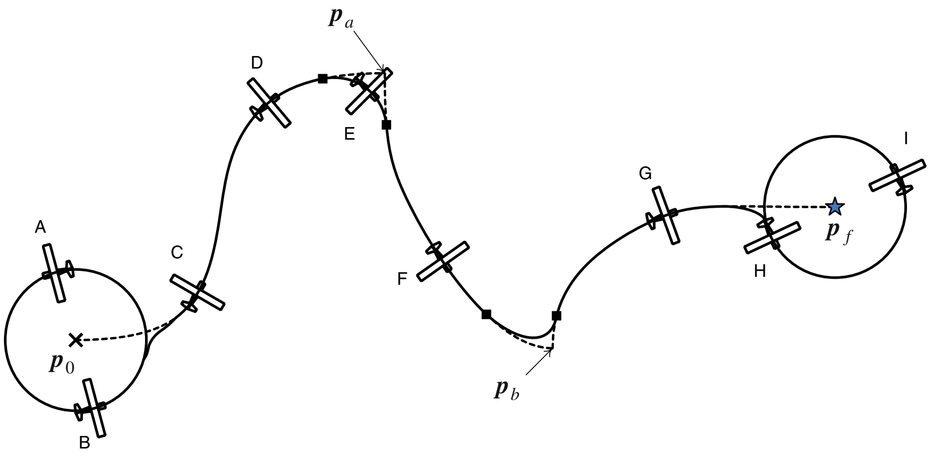

Step	Task description
A	Initially, the UAV is loitering around the initial position with the circle radius R_l
B	Calculate the first path segment from $\boldsymbol{p}_0$ to $\boldsymbol{p}_a$
C	Break away from the loitering circle, start to follow the first path segment
D	Calculate the second segment from $\boldsymbol{p}_a$ to $\boldsymbol{p}_b$, and a transient path
E	UAV is on the transient path
F	Calculate the third path segment, and a transient path
G	UAV is approaching the goal position, no path is calculated
H	The goal is reached, end of the path control, get on the loitering circle
I	UAV is loitering around the goal position $\boldsymbol{p}_f$

Fig. 8 Illustration of the real-time implementation of the proposed hierarchical path planning and control algorithm

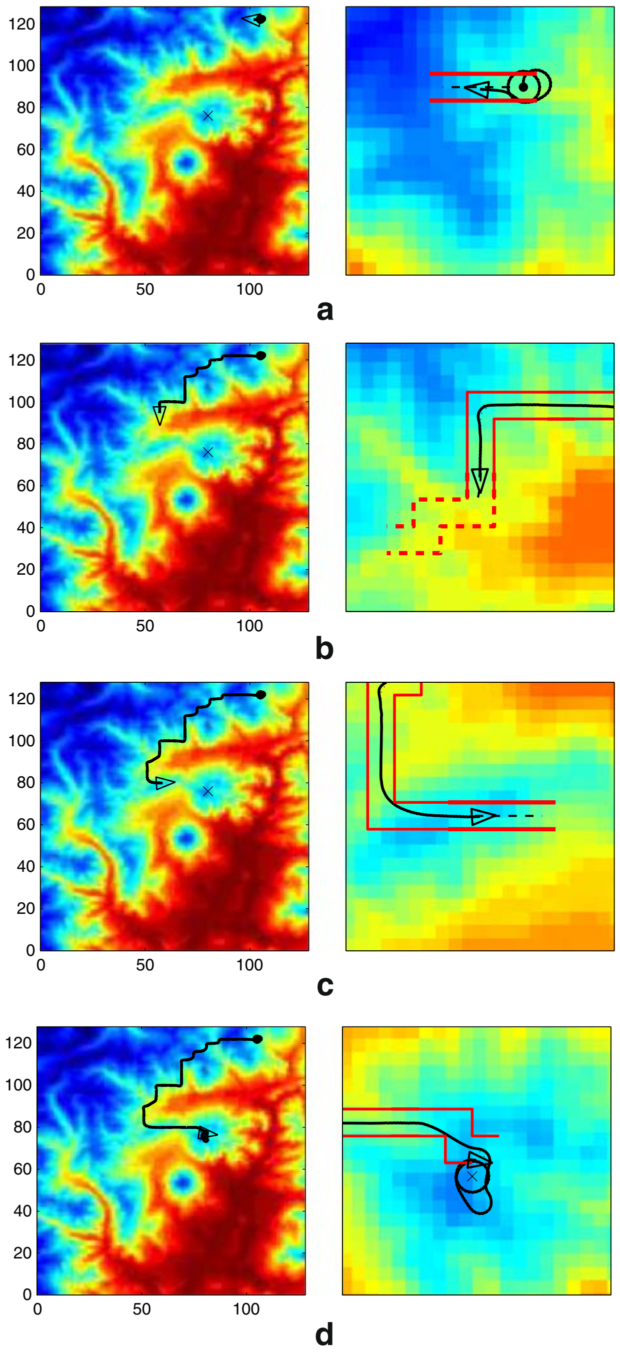

Fig. 9 HILS results of the hierarchical path planning and control implementation. The *plots on the right* show the close-up view of the simulation. At each instant, the channel where the smooth path segment from the corresponding path template has to stay, is drawn by polygonal lines. The actual path followed by the UAV is drawn on top of the reference path. **a** $t = 64.5$ s. **b** $t = 333.0$ s. **c** $t = 429.0$ s. **d** $t = 591.5$ s

$\boldsymbol{p}_a$ to the goal, resulting in the second local path segments from $\boldsymbol{p}_a$ to $\boldsymbol{p}_b$. The first and second path segments are stitched by a transient B-spline path assuring the continuity condition at each intersection point (marked by black squares). This process iterates until the final position $\boldsymbol{p}_f$ is reached (Step H), when the UAV engages to loitering around the goal location.

5.2 Simulation Results

Figure 9 shows the simulation results of the hierarchical path planning and control implementation. Specifically, the plots on the right show the close-up view of the simulation. The channels are drawn by solid polygonal lines. The actual trajectory followed by the UAV is also shown. The UAV smoothly follows the reference path while avoiding all possible obstacles outside these channels. Finally, the UAV reaches the final destination in a collision-free manner, as seen in Fig. 9d.

5.3 Real-Time Kernel Run-Time Statistics

In order to evaluate the performance of the real-time software framework, we have used several distinct metrics that are available within the real-time kernel.

The amount of time for which the CPU is utilized by the kernel and task execution can be retrieved from the CPU usage metric, which is the percentage of the duty cycle of the CPU, provided by the real-time kernel at every second. When high CPU demanding tasks such as PPLAN and PGEN get activated, a higher percentage of CPU usage implies quicker completion of these tasks. Consequently, a higher percentage of CPU usage implies higher performance and efficiency. Figure 10a shows this metric during the simulation. It is noticed that for most of the time the CPU usage is about 40%, however, when a new path segment needs to be calculated (see Step D and F in Fig. 8), it goes up to nearly 100%, until the tasks PPLAN and PGEN are completed and can provide a new reference curve.

Context switches are performed when the real-time scheduler needs to switch from the current task to a different task. Each context switch is comprised of storing the current CPU register, restoring the CPU register from the stack of the new task, and resuming execution of the new task's code. Subsequently, this operation adds overhead to the existing application, which should be kept at a minimum. The number of context switches per second is provided by the real-time kernel and helps keep track of the system overhead. Although the performance of the real-time kernel should not be justified by this number, this metric can be interpreted as an indication of the health status of the real-time software. In other words, increased overhead may cause the scheduler to delay switching and make tasks be activated out of their proper timing due to this latency. If this happens, because the number of context switches represents the system overhead, hence it reveals the health status of the system. Figure 10b shows the number of context switches per second during our experiments. Given the sampling period of $T_s = 50$ ms, we notice that the average number of context switches per each sampling period is approximately seven. This indicates that the overhead is relatively small, taking into account the number of routine tasks that should be completed during each sampling period.

Individual task execution time is measured during run-time, by referencing a hook function `OSTaskSwHook()` when a context switching is performed. This function calculates the elapsed CPU time of the preempted task and updates a task-specific data structure with this information. Subsequently, when a statistics hook function is

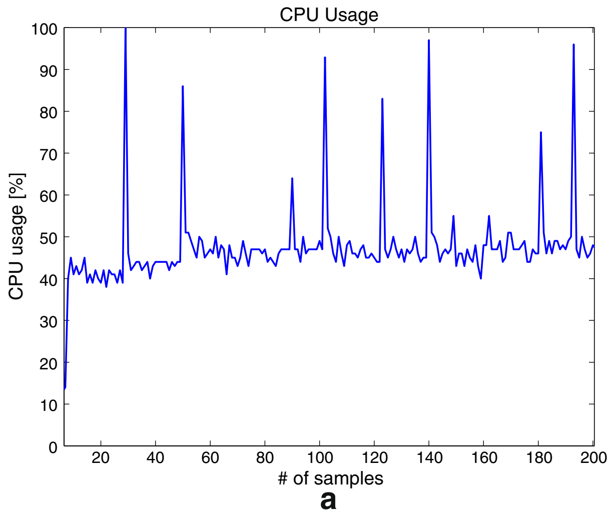

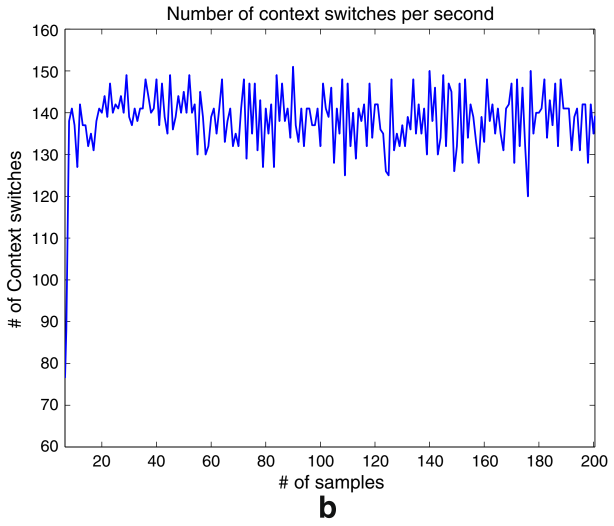

Fig. 10 Real-time kernel run-time statistics: CPU usage (**a**) and number of context switches per second (**b**)

called by the real-time kernel, each task execution time $\texttt{TET}_i(k)$ is added together to get the total execution time of all tasks. On the other hand, the CPU ratio of different tasks, i.e., the percentage of time actually consumed by each task, is computed as follows,

$$\pi_i(k) = \frac{\texttt{TET}_i(k)}{\sum_{i=1}^{N} \texttt{TET}_i(k)} \times 100 \quad [\%], \tag{1}$$

where $\pi_i(k)$ denotes a percentage of time consumed by ith task at kth time. Figure 11a shows the run-time CPU ratio. Different colors are used to distinguish between different tasks, as depicted by the colorbar on the right side of each figure.

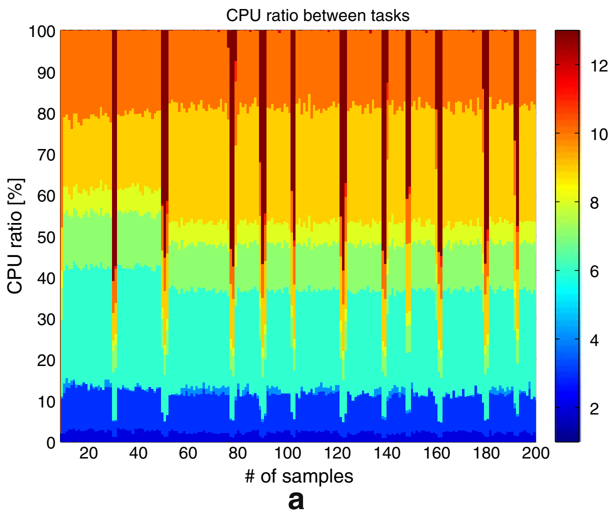

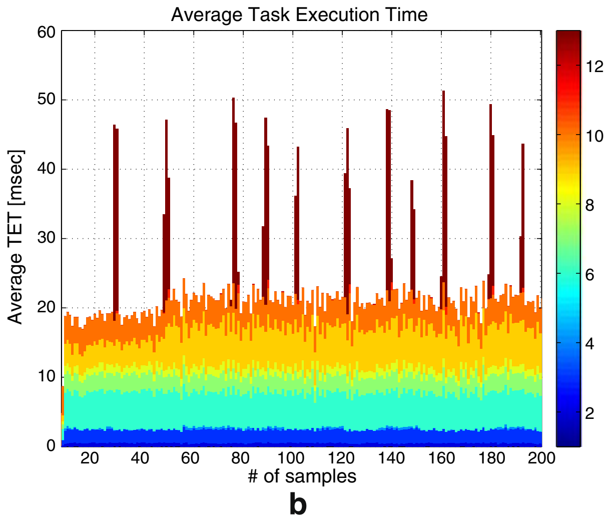

Fig. 11 Real-time kernel run-time statistics: CPU ratio over different tasks (**a**) vs. Mean tasks execution time (**b**)

Finally, the execution time of each task over the given sampling period $T_s = 50$ ms is calculated as follows,

$$\overline{\mathtt{TET}}_i(k) = \frac{\mathtt{TET}_i(k)}{(t_k - t_{k-1})/T_s} \quad [\text{ms}], \tag{2}$$

where t_k denotes the actual time of the kth statistical sample. Equation 2 basically calculates the mean value of the execution time of the ith task over one sampling period. This metric is updated at every statistical sample. As shown in Fig. 11b, this metric helps us check if the total sum of execution times of different tasks exceeds the given sampling period T_s.

6 Conclusions

We have implemented a hierarchical path planning and control algorithm of a small UAV on the actual hardware platform. Using a high fidelity HIL simulation environment, the proposed hierarchical path planning and control algorithm has been validated through the on-line, real-time implementation on a small autopilot. By integrating the control algorithms for path planning, path smoothing, and path following under two real-time/near real-time implementations, it has been demonstrated that the UAV equipped with a small autopilot having limited computational resources manages to accomplish the mission objective of reaching the goal destination, while avoiding obstacles. Emphasizing the use of a real-time kernel, we have discussed the implementation issues utilizing the kernel services, which allows flexibility of task management, robustness of code execution, etc. Provided with quantitative metrics, we have shown that the real-time kernel successfully accomplishes real-time operation of a small UAV for a non-trivial, realistic, path planning scenario.

Acknowledgements Partial support for this work has been provided by NSF award no. CMS-0510259 and NASA award no. NNX08AB94A.

References

1. Balluchi, A., Berardi, L., Di Benedetto, M., Ferrari, A., Girasole, G., Sangiovanni-Vincentelli, A.L.: Integrated control-implementation design. In: Proceedings of the 41st IEEE Conference on Decision and Control, pp. 1337–1342. IEEE, Las Vegas, December 2002
2. Beard, R.W., McLain, T.W., Goodrich, M., Anderson, E.P.: Coordinated target assignment and intercept for unmanned air vehicles. IEEE Trans. Robot. Autom. **18**, 911–922 (2002)
3. Bellingham, J., Richards, A., How, J.: Receding horizon control of autonomous aerial vehicles. In: Proceedings of the American Control Conference, pp. 3741–3745, Anchorage, May 2002
4. Bortoff, S.A.: Path planning for UAVs. In: Proceedings of the American Control Conference, pp. 364–368, Chicago, June 2000
5. Chandler, P., Pachter, M.: Research issues in autonomous control of tactical UAVs. In: Proceedings of the American Control Conference, Philadelphia, June 1998
6. Christophersen, H.B., Pickell, R.W., Neidhoefer, J.C., Koller, A.A., Kannan, S.K., Johnson, E.N.: A compact guidance, navigation, and control system for unmanned aerial vehicles. J. Aerosp. Comput. Inf. Commun. **3**(5), 187–213 (2006)
7. Gelperin, D.: On the optimality of A*. Artif. Intell. **8**(1), 69–76 (1977)
8. Hall, C.: On board flight computers for flight testing small uninhabited aerial vehicles. In: The 2002 45th Midwest Symposium on Circuits and Systems, vol. 2, pp. II-139–II-143. IEEE, August 2002
9. Hart, P., Nilsson, N., Rafael, B.: A formal basis for the heuristic determination of minimum cost paths. IEEE Trans. Sys. Sci. Cybern. **4**, 100–107 (1968)
10. Jang, J., Tomlin, C.: Autopilot design for the Stanford DragonFly UAV: validation through hardware-in-the-loop simulation. In: AIAA Guidance, Navigation, and Control Conference, AIAA 2001–4179, Montreal, August 2001
11. Jang, J., Tomlin, C.: Design and implementation of a low cost, hierarchical and modular avionics architecture for the DranfonFly UAVs. In: AIAA Guidance, Navigation, and Control Conference and Exhibit, AIAA 2002-4465, Monterey, August 2002
12. Jang, J.S., Liccardo, D.: Small UAV automation using MEMS. IEEE Aerosp. Electron. Syst. Mag. **22**(5), 30–34 (2007)
13. Jang, J.S., Tomlin, C.: Longitudinal stability augmentation system design for the DragonFly UAV using a single GPS receiver. In: AIAA Guidance, Navigation, and Control Conference, AIAA 2003-5592, Austin, August 2003

14. Jang, J.S., Tomlin, C.J.: Design and implementation of a low cost, hierarchical and modular avionics architecture for the dragonfly UAVs. In: AIAA Guidance, Navigation, and Control Conference and Exhibit, Monterey, August 2002
15. Johnson, E.N., Proctor, A.A., Ha, J., Tannenbaum, A.R.: Development and test of highly autonomous unmanned aerial vehicles. J. Aerosp. Comput. Inf. Commun. **1**, 486–500 (2004)
16. Jung, D.: Hierarchical path planning and control of a small fixed-wing UAV: theory and experimental validation. Ph.D. thesis, Georgia Institute of Technology, Atlanta, GA (2007)
17. Jung, D., Levy, E.J., Zhou, D., Fink, R., Moshe, J., Earl, A., Tsiotras, P.: Design and development of a low-cost test-bed for undergraduate education in uavs. In: Proceedings of the 44th IEEE Conference on Decision and Control, pp. 2739–2744. IEEE, Seville, December 2005
18. Jung, D., Tsiotras, P.: Inertial attitude and position reference system development for a small uav. In: AIAA Infotech at Aerospace, AIAA 07-2768, Rohnert Park, May 2007
19. Jung, D., Tsiotras, P.: Modelling and hardware-in-the-loop simulation for a small unmanned aerial vehicle. In: AIAA Infotech at Aerospace, AIAA 07-2763, Rohnert Park, May 2007
20. Jung, D., Tsiotras, P.: Bank-to-turn control for a small UAV using backstepping and parameter adaptation. In: International Federation of Automatic Control (IFAC) World Congress, Seoul, July 2008
21. Jung, D., Tsiotras, P.: Multiresolution on-line path planning for small unmanned aerial vehicles. In: American Control Conference, Seattle, June 2008
22. Jung, D., Tsiotras, P.: On-line path generation for small unmanned aerial vehicles using B-spline path templates. In: AIAA Guidance, Navigation and Control Conference, AIAA 2008-7135, Honolulu, August 2008
23. Kaminer, I., Yakimenko, O., Dobrokhodov, V., Lim, B.A.: Development and flight testing of GNC algorithms using a rapid flight test prototyping system. In: AIAA Guidance, Navigation, and Control Conference and Exhibit, Monterey, August 2002
24. Kingston, D., Beard, R.W., McLain, T., Larsen, M., Ren, W.: Autonomous vehicle technologies for small fixed wing UAVs. In: 2nd AIAA Unmanned Unlimited Conference and Workshop and Exhibit, Chicago 2003
25. Kingston, D.B., Beard, R.W.: Real-time attitude and position estimation for small UAVs using low-cost sensors. In: AIAA 3rd Unmanned Unlimited Technical Conference, Workshop and Exhibit, Chicago, September 2004
26. Labrosse, J.J.: MicroC/OS-II - The Real-Time Kernel, 2nd edn. CMPBooks, San Francisco (2002)
27. McLain, T., Chandler, P., Pachter, M.: A decomposition strategy for optimal coordination of unmanned air vehicles. In: Proceedings of the American Control Conference, pp. 369–373, Chicago, June 2000
28. McLain, T.W., Beard, R.W.: Coordination variables, coordination functions, and cooperative timing missions. J. Guid. Control Dyn. **28**(1), 150–161 (2005)
29. Palopoli, L., Pinello, C., Sangiovanni-Vincentelli, A.L., Elghaoui, L., Bicchi, A.: Synthesis of robust control systems under resource constraints. In: HSCC '02: Proceedings of the 5th International Workshop on Hybrid Systems: Computation and Control, pp. 337–350. Stanford, March 2002
30. Tsiotras, P., Bakolas, E.: A hierarchical on-line path planning scheme using wavelets. In: Proceedings of the European Control Conference, pp. 2806–2812, Kos, July 2007